# First Measurement of $\nu_\mu$ and $\nu_e$ Events in an Off-Axis Horn-Focused Neutrino Beam

P. Adamson,[8] A. A. Aguilar-Arevalo,[6] C. E. Anderson,[22] A. O. Bazarko,[15] M. Bishai,[2] S. J. Brice,[8] B. C. Brown,[8] L. Bugel,[6] J. Cao,[13] B. C. Choudhary,[8] L. Coney,[6] J. M. Conrad,[14] D. C. Cox,[10] A. Curioni,[22] Z. Djurcic,[6] D. A. Finley,[8] B. T. Fleming,[22] R. Ford,[8] H. R. Gallagher,[18] F. G. Garcia,[8] G. T. Garvey,[11] C. Green,[11,8] J. A. Green,[10,11] D. Harris,[8] T. L. Hart,[5] E. Hawker,[20] J. Hylen,[8] R. Imlay,[12] R. A. Johnson,[4] G. Karagiorgi,[14] P. Kasper,[8] T. Katori,[10] T. Kobilarcik,[8] S. Kopp,[17] I. Kourbanis,[8] S. Koutsoliotas,[3] E. M. Laird,[15] S. K. Linden,[22] J. M. Link,[19] Y. Liu,[13] Y. Liu,[1] L. Loiacono,[17] W. C. Louis,[11] A. Marchionni,[8] K. B. M. Mahn,[6] W. Marsh,[8] G. McGregor,[11] M. D. Messier,[10] W. Metcalf,[12] P. D. Meyers,[15] F. Mills,[8] G. B. Mills,[11] J. Monroe,[14] C. D. Moore,[8] J. K. Nelson,[21] R. H. Nelson,[5] V. T. Nguyen,[14] P. Nienaber,[16] J. A. Nowak,[12] S. Ouedraogo,[12] R. B. Patterson,[15] Z. Pavlovic,[17] D. Perevalov,[1] C. C. Polly,[10] E. Prebys,[8] J. L. Raaf,[4] H. Ray,[11,9] B. P. Roe,[13] A. D. Russell,[8] V. Sandberg,[11] R. Schirato,[11] D. Schmitz,[6] M. H. Shaevitz,[6] F. C. Shoemaker,[15] W. Smart,[8] D. Smith,[7] M. Sodeberg,[22] M. Sorel,[6] P. Spentzouris,[8] I. Stancu,[1] R. J. Stefanski,[8] M. Sung,[12] H. A. Tanaka,[15] R. Tayloe,[10] M. Tzanov,[5] P. Vahle,[21] R. Van de Water,[11] B. Viren,[2] M. O. Wascko,[12,*] D. H. White,[11] M. J. Wilking,[5] H. J. Yang,[13] F. X. Yumiceva,[21] G. P. Zeller,[6,11] E. D. Zimmerman,[5] and R. Zwaska[8]

[1] *University of Alabama; Tuscaloosa, AL 35487*
[2] *Brookhaven National Laboratory; Upton, NY 11973*
[3] *Bucknell University; Lewisburg, PA 17837*
[4] *University of Cincinnati; Cincinnati, OH 45221*
[5] *University of Colorado; Boulder, CO 80309*
[6] *Columbia University; New York, NY 10027*
[7] *Embry-Riddle Aeronautical University; Prescott, AZ 86301*
[8] *Fermi National Accelerator Laboratory; Batavia, IL 60510*
[9] *University of Florida; Gainesville, FL 32611*
[10] *Indiana University; Bloomington, IN 47405*
[11] *Los Alamos National Laboratory; Los Alamos, NM 87545*
[12] *Louisiana State University; Baton Rouge, LA 70803*
[13] *University of Michigan; Ann Arbor, MI 48109*
[14] *Massachusetts Institute of Technology; Cambridge, MA 02139*
[15] *Princeton University; Princeton, NJ 08544*
[16] *Saint Mary's University of Minnesota; Winona, MN 55987*
[17] *University of Texas; Austin, TX 78712*
[18] *Tufts University; Medford, MA 02155*
[19] *Virginia Polytechnic Institute & State University; Blacksburg, VA 24061*
[20] *Western Illinois University; Macomb, IL 61455*
[21] *College of William & Mary; Williamsburg, VA 23187*
[22] *Yale University; New Haven, CT 06520*

(Dated: July 24, 2009)



We report the first observation of off-axis neutrino interactions in the MiniBooNE detector from the NuMI beamline at Fermilab. The MiniBooNE detector is located 745 m from the NuMI production target, at 110 mrad angle (6.3°) with respect to the NuMI beam axis. Samples of charged current quasi-elastic $\nu_\mu$ and $\nu_e$ interactions are analyzed and found to be in agreement with expectation. This provides a direct verification of the expected pion and kaon contributions to the neutrino flux and validates the modeling of the NuMI off-axis beam.

PACS numbers: 25.30.Pt, 13.15.+g, 14.60.Lm, 14.60.Pq

Conventional neutrino beams from high-energy proton accelerators serve as important tools for studying neutrino characteristics and the fundamental properties of matter involving interactions of neutrinos. Such beams typically arise from the two-body decays of $\pi$ and $K$ mesons produced by a proton beam impinging upon a nuclear target. The mesons leave the target with a significant angular divergence. The flux of neutrinos in such a wide band beam at distance $d$ from the meson decay point and at an angle $\theta$ with respect to the parent meson direction is given by

$$\Phi_\nu \approx \frac{1}{4\pi d^2}\Big(\frac{2\gamma}{1+\gamma^2\theta^2}\Big)^2, \tag{1}$$

where $\gamma$ is the Lorentz boost factor of mesons [1]. To obtain a more intense neutrino flux, it is essential to focus the mesons produced in the target. To accomplish this, neutrino experiments such as MiniBooNE [2] and MINOS [3] use focusing magnetic horns to direct the mesons toward downstream detectors. The energy of $\nu_\mu$s

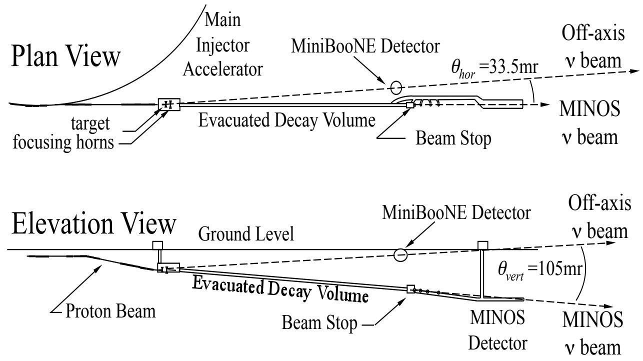


FIG. 1: Plan and elevation views of the NuMI beamline with respect to the MiniBooNE detector.

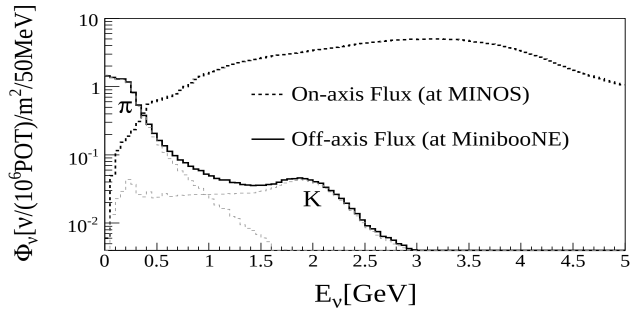


FIG. 2: Comparison of the predicted NuMI off-axis and on-axis fluxes including all neutrino species. The off-axis flux is separated into contributions from charged $\pi$ and $K$ parents.

from two-body decays is given by

$$E_\nu \approx \frac{\left(1 - \frac{m_\mu^2}{m_{\pi,K}^2}\right) E_{\pi,K}}{1 + \gamma^2 \tan^2\theta}, \quad (2)$$

where $m_{\pi,K}$ ($E_{\pi,K}$) is the mass (energy) of the $\pi$, $K$ parent, and $m_\mu$ is the muon mass. Brookhaven experiment E889 proposed [4] an off-axis beam because, at a suitable off-axis angle $\theta$, the neutrino flux is confined to a relatively narrow band of energies, which is useful in limiting backgrounds in searches for the oscillation transition $\nu_\mu \rightarrow \nu_e$. Future neutrino oscillation searches by the T2K [5] and NO$\nu$A [6] experiments plan to use off-axis horn-focused beams.

The MiniBooNE detector, located at an angle of 110 mrad (6.3°) with respect to the NuMI beam axis (see Fig. 1), provides a unique opportunity to perform the first measurement of neutrino interactions from an off-axis horn-focused beam. In addition to demonstrating the off-axis beam concept, the measurement verifies the predicted fluxes from $\pi/K$ parents in the NuMI beam, and probes the off-axis intrinsic $\nu_e$ contamination, required for future $\nu_\mu \rightarrow \nu_e$ appearance searches.

The NuMI beam points toward the MINOS Far Detector, located in the Soudan Laboratory in Minnesota. Neutrinos are produced by 120 GeV protons incident on a carbon target. In the period studied here, the beam intensity was up to $3 \times 10^{13}$ protons on target per spill at a typical repetition rate of 0.48 Hz. Positive $\pi$ and $K$ mesons produced in the target are focused down the decay pipe using two magnetic horns. Neutrinos from two-body decays of pions are more forward directed than those from kaons due to the difference in rest mass of the decaying mesons. As a result, the off-axis component coming from pions is suppressed relative to the kaon component. Decay in flight of poorly focused pions can only occur close to the NuMI target, since they are stopped by shielding around the target area. The NuMI beam also provides a large sample of $\nu_e$ events in the MiniBooNE detector. The $\nu_e$'s result primarily from the three-body decay of kaons and thus have a wider range of energies.

Detailed GEANT3-based [7] Monte Carlo (MC) simulations of the beam, including secondary particle production, particle focusing, and transport, are performed to calculate the flux as a function of neutrino flavor and energy. The yield of pions and kaons from the NuMI target is calculated using the FLUKA cascade model [8]. The beam modeling includes downstream interactions in material other than the target that produce hadrons decaying to neutrinos. These interactions are modeled using a GEANT3 simulation, configured to use either GFLUKA [7] or GCALOR [9] cascade models. The NuMI neutrino flux at the MiniBooNE detector is shown in Fig. 2. Pions (kaons) produce neutrinos with average energies of about 0.25 GeV (2 GeV).

These neutrinos are detected in the MiniBooNE detector [10] which is a 12.2 m spherical tank filled with 800 tons of pure mineral oil. The detector triggers on every NuMI beam spill and the detector activity is recorded in a 19.2 $\mu s$ window beginning about 1 $\mu s$ before the start of a $\sim$10 $\mu s$ wide spill. The time and charge of photomultiplier-tubes (PMT) in the detector are used to reconstruct the interaction point, event time, energies, and particle tracks resulting from neutrino interactions. Neutrino interactions in the detector are simulated with the NUANCE event generator package [11], with modifications to the quasi-elastic (QE) cross-section as described in [12]. Particles generated by NUANCE are propagated through the detector, using a GEANT3-based simulation which describes the emission of optical and near-UV photons via Cherenkov radiation and scintillation. Neutrino induced events are identified by requiring the event to occur during the NuMI beam spill, after rejection of cosmic ray muons and muon decay electrons [2]. For the sample satisfying these selection criteria, NuMI neutrinos are predicted to interact via charged-current (CC) QE scattering (39%), CC single pion production (31%), neutral current (NC) single pion production (14%), multi-pion production (9%), deep inelastic scattering (4%), and other interactions (3%). The predicted event composition is $\nu_\mu : \bar{\nu}_\mu : \nu_e : \bar{\nu}_e \sim 0.81 :$

0.13 : 0.05 : 0.01.

The data set analyzed here corresponds to $1.42 \times 10^{20}$ protons delivered to the NuMI target from June 22, 2005 to March 2, 2007. The MC in all cases has been normalized to this number of protons. Neutrino interactions are identified with the likelihood-based algorithm used in [2].

The high rate and simple topology of $\nu_\mu$ CCQE events provides a useful sample for understanding the $\nu_\mu$ spectrum and verifying the MC prediction for $\nu_e$ production. The identification of $\nu_\mu$ CCQE events is based upon the detection of the primary stopping muon and the associated decay electron as two distinct time-related clusters of PMT hits, called 'subevents': $\nu_\mu + n \rightarrow \mu^- + p, \quad \mu^- \rightarrow e^- + \nu_\mu + \bar{\nu}_e$. We require the first subevent to have a reconstructed position within 5 m of the center of the detector. The decay electron requirement substantially reduces CC single $\pi^+$ contamination because most CC $\pi^+$ events contain a second decay electron from the $\pi^+$ to $\mu$ decay chain. Additional rejection of non-$\nu_\mu$ CCQE events in the sample is achieved by a requirement on the relative $\mu$ and e likelihoods, maximized under a given particle hypothesis, $\log(L_e/L_\mu) < 0.02$. This selection criterion is 24% efficient in selecting $\nu_\mu$ CCQE candidates, resulting in a 69% pure $\nu_\mu$ CCQE sample. The most significant background contribution to the $\nu_\mu$ CCQE sample result from CC single $\pi^+$ production (78%) where the $\pi^+$ is undetected. A total of 17452 data events pass this $\nu_\mu$ CCQE selection criteria, compared to the prediction of 18545±3240; the uncertainty includes systematic errors associated with the neutrino flux, neutrino cross-sections, and detector modeling. The flux uncertainties include particle production in the NuMI target, modeling of the downstream interactions, and kaons stopped in the NuMI beam dump. The $\pi/K$ yields were tuned to match the MINOS Near Detector data [3] in several of the NuMI beam configurations. Such tuning has a negligible effect on the off-axis beam at MiniBooNE. However, the difference between untuned and tuned $\pi/K$ yields is treated as an additional systematic effect. The cross-section uncertainties are quantified by varying the underlying model parameters constrained by either external or Booster neutrino beam (BNB) data. Uncertainties in the parameters describing the optical properties of the MiniBooNE detector are constrained by external measurements of the oil properties and by fits to calibration samples of events in the BNB data sample [2].

Reconstructed $\nu_\mu$ CCQE event kinematics include the muon energy, $E_\mu$, and muon angle with respect to the neutrino beam direction, $\theta_\mu$. For both the data and MC, $\theta_\mu$ is approximated assuming that all neutrinos arise from meson decays at the NuMI production target. In reality, mesons decay along the NuMI beamline so that the average decay distance from the target is about 70 m. However, given the geometry of the beamline with respect to the detector (see Fig. 1), such an off-axis angle change is well within the angular resolution of the detector ($\sim 2°$).

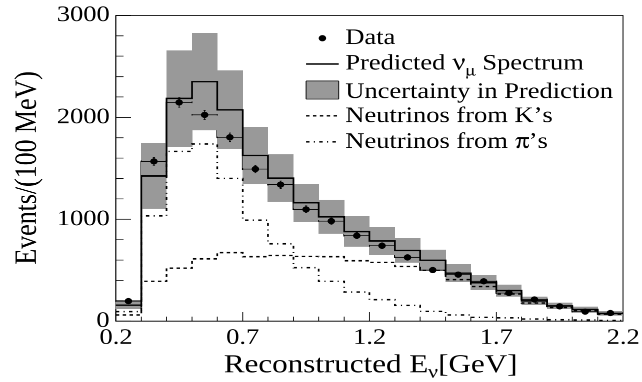


FIG. 3: Reconstructed $E_\nu$ distribution of $\nu_\mu$ CCQE events. The band indicates the total systematic uncertainty associated with the MC prediction. Also shown are the contributions from pion (52%) and kaon (48%) parents of neutrinos.

TABLE I: Observed and predicted $\nu_\mu$-like events in two energy bins. The predicted events are further separated into contributions from kaon and pion parents of neutrinos.

| $E_\nu$ [GeV] | Data | MC Prediction | $\pi$ | $K$ |
|---|---|---|---|---|
| 0.2-0.9 | 10586±103 | 11231±2156 | 7655 | 3576 |
| 0.9-2.2 | 6866± 83 | 7314±1221 | 1949 | 5365 |

Based on these reconstructed quantities, the neutrino energy, $E_\nu$, is calculated assuming two-body kinematics

$$E_\nu = \frac{1}{2} \frac{2M_p E_\mu - m_\mu^2}{M_p - E_\mu + \sqrt{(E_\mu^2 - m_\mu^2)} \cos\theta_\mu}, \qquad (3)$$

where $M_p$ is the proton mass. The $E_\nu$ resolution of NuMI neutrinos in MiniBooNE is $\sim 12\%$ at 1 GeV. The $E_\nu$ distribution of selected $\nu_\mu$ CCQE events is shown in Fig. 3, along with the MC prediction, separated into pion and kaon contributions. Predicted pion and kaon contributions, in two energy regions, are given in Table I. Systematic uncertainties of the predicted event rates are given in Table II. The agreement between data and the prediction of the neutrino flux from $\pi/K$ parents indicates that the NuMI beam modeling provides a good description of the observed off-axis $\nu_\mu$ flux in MiniBooNE.

TABLE II: Systematic uncertainties of the predicted event rate in the full energy range and in two $E_\nu$ bins, for CCQE $\nu_\mu$ and $\nu_e$ samples.

| Event Sample | Systematic Error Component | 0.2-3.0 | $E_\nu$ [GeV] 0.2-0.9 | 0.9-3.0 |
|---|---|---|---|---|
| $\nu_\mu$ | Flux [%] | 9.2 | 11.9 | 4.7 |
| | Cross-sec. [%] | 14.6 | 14.7 | 15.4 |
| | Detector [%] | 3.1 | 3.2 | 4.4 |
| | Total [%] | 17.5 | 19.2 | 16.7 |
| $\nu_e$ | Flux [%] | 7.2 | 8.3 | 5.6 |
| | Cross-sec. [%] | 14.2 | 14.2 | 15.2 |
| | Detector [%] | 5.6 | 7.9 | 5.0 |
| | Total [%] | 17.0 | 18.3 | 17.1 |

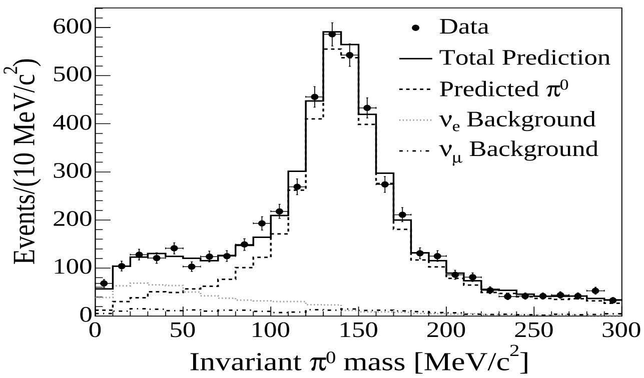


FIG. 4: Mass distribution of NC $\pi^0$ candidates for data (points) and MC (solid histogram). The dashed histogram is the subset of predicted events with at least one true $\pi^0$. Predicted non-$\pi^0$ backgrounds are either from $\nu_\mu$ and $\bar{\nu}_\mu$ (dash-dotted line) or $\nu_e$ and $\bar{\nu}_e$ (dotted line) interactions. Kaon parents contribute 84% of the events in this sample.

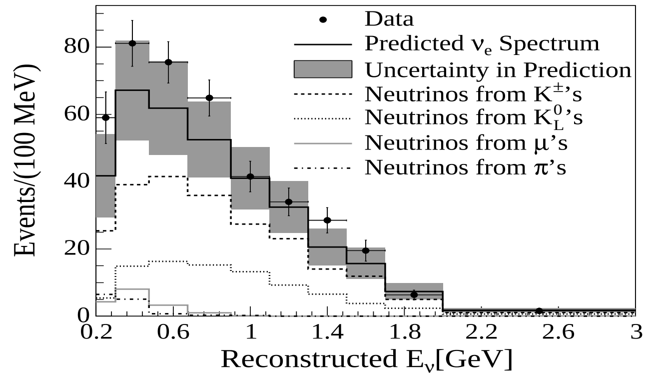


FIG. 5: Reconstructed $E_\nu$ distribution of $\nu_e$ CCQE candidates. The prediction is separated into contributions from neutrino parents. The band indicates the total systematic uncertainty associated with the MC prediction. Kaon parents contribute 93% of the events in this sample.

The $\nu_e$ CCQE events consist of a single subevent of PMT hits ($\nu_e{+}n \rightarrow e^-{+}p$). In 8% of $\nu_\mu$ CCQE events the $\mu^-$ is captured on carbon, resulting in a single subevent. These events are removed with an energy dependent requirement on the likelihood ratio, $\log(L_e/L_\mu)$. The majority of the remaining background is NC $\pi^0$ events with only a single reconstructed electromagnetic track that mimics a $\nu_e$ CCQE event. To test our NC $\pi^0$ prediction, a clean sample of NC $\pi^0$ events is reconstructed, as shown in Fig. 4. This sample demonstrates good agreement between data and MC. The majority of $\pi^0$ events in the $\nu_e$ CCQE sample are rejected by requirements on the reconstructed $\pi^0$ mass and the electron to pion likelihood ratio, applied as a function of visible energy.

A source of low energy $\nu_e$ events arises from the decay of stopped kaons in the beam stop at the end of the NuMI beamline, which is under the MiniBooNE detector (see Fig. 1), 83 m from its center. Given the kinematics of stopped kaon decay, all $\nu_e$'s from this source will have visible energies ($E_e$) below 200 MeV. A requirement $E_e > 200$ MeV effectively removes this source. A total of 780 data events pass all of the $\nu_e$ CCQE selection criteria. The MC prediction is 660±112 with a $\nu_e$ CCQE efficiency of 32% and purity of 70%. The corresponding energy distribution is shown in Fig. 5, and the uncertainties on the predicted event rate are given in Table II. To facilitate further comparison, the low and high energy regions are divided at 0.9 GeV, and the numbers of data and MC events in these two regions provided in Table III. The data with $E_\nu < 0.9$ GeV are systematically above the prediction at the 1.25 $\sigma$ level.

In summary, we have presented the first observation and analysis of neutrino interactions with an off-axis horn-focused neutrino beam. The agreement between data and prediction in the $\nu_\mu$ and $\nu_e$ CCQE samples

TABLE III: Observed and predicted $\nu_e$-like events in two energy bins. The predicted events are further separated into intrinsic $\nu_e$ (and $\bar{\nu}_e$) and $\nu_\mu$ (and $\bar{\nu}_\mu$) components.

| $E_\nu$[GeV] | Data | MC Prediction | $\nu_e{+}\bar{\nu}_e$ | $\nu_\mu{+}\bar{\nu}_\mu$ |
|---|---|---|---|---|
| 0.2-0.9 | 498±22 | 401±74 | 311 | 90 |
| 0.9-3.0 | 282±17 | 259±45 | 231 | 28 |

demonstrates good understanding of both pion and kaon contributions to the beam. This represents a successful demonstration of an off-axis neutrino beam at 110 mrad and provides a clear proof-of-principle of the off-axis beam concept planned for use in future neutrino experiments.

We acknowledge the support of Fermilab, the Department of Energy, and the National Science Foundation.

* Present address: Imperial College London, London, UK

[1] S. Kopp, Phys. Rep. **439**, 101 (2007).
[2] A. A. Aguilar-Arevalo *et al.*, Phys. Rev. Lett. **98**, 231801 (2007).
[3] P. Adamson *et al.*, Phys. Rev. D **77**, 072002 (2008).
[4] D. Beavis *et al.*, Report. No. BNL-52459 (1995).
[5] Y. Itow *et al.*, arXiv:hep-ex/0106019.
[6] D. Ayres *et al.*, FERMILAB-DESIGN-2007-01.
[7] CERN Program Library Long Writeup W5013 (1993).
[8] A. Fasso *et al.*, CERN-2005-10, INFN/TC_05/11, SLAC-R-773 (2005).
[9] C. Zeitnitz and T. A. Gabriel, Nucl. Instrum. Meth. A **349**, 106 (1994).
[10] A. A. Aguilar-Arevalo *et al.*, arXiv:0806.4201 [hep-ex].
[11] D. Casper, Nucl. Phys. Proc. Suppl. **112**, 161 (2002).
[12] A. A. Aguilar-Arevalo *et al.*, Phys. Rev. Lett. **100**, 032301 (2008).